

# U.S. CONTRIBUTION TO THE INTERNATIONAL TOKAMAK REACTOR WORKSHOP, PHASE 2A, PART 3, 1985-1987

W. M. STACEY, Jr. *Georgia Institute of Technology  
Nuclear Engineering and Health Physics Programs  
Engineering Science and Mechanics Building, Atlanta, Georgia 30332*

DAVID A. EHST *Argonne National Laboratory  
9700 S. Cass Avenue, Argonne, Illinois 60440*

CHARLES A. FLANAGAN and Y.-K. MARTIN PENG  
*Oak Ridge National Laboratory, Fusion Engineering Design Center  
P.O. Box Y, Oak Ridge, Tennessee 37830*

N. POMPHREY and DOUGLASS E. POST  
*Princeton University, Plasma Physics Laboratory  
P.O. Box 451, Princeton, New Jersey 08540*

DALE L. SMITH *Argonne National Laboratory  
9700 S. Cass Avenue, Argonne, Illinois 60440*

P. T. SPAMPINATO *Oak Ridge National Laboratory  
Fusion Engineering Design Center, P.O. Box Y, Oak Ridge, Tennessee 37830*

Received July 15, 1988

Accepted for Publication December 1, 1988

*The recent phase of the International Tokamak Reactor Workshop focused on the analysis of critical technical issues, evaluation of innovations, analysis of national engineering test reactor designs, and assessment of the supporting data base for a tokamak engineering test reactor.*

## I. INTRODUCTION

The International Tokamak Reactor (INTOR) Workshop was initiated in 1979 as a collaborative effort among the European Communities, Japan, the United States, and the USSR, to be conducted under the auspices of the International Atomic Energy Agency (IAEA), under terms defined by the International Fusion Research Council (IFRC), an advisory body to the director general of the IAEA, which supervises the INTOR Workshop. The broad objectives as set

forth by the IFRC were to draw on worldwide capability to

1. identify the objectives and characteristics of the next major experiment (beyond the present generation of large tokamaks) in the world tokamak program
2. assess the technical data base that will exist to support the construction of such a device for operation in the 1990s
3. define such an experiment through the development of a conceptual design
4. study critical technical issues that affect the feasibility or cost of the INTOR concept
5. define research and development (R&D) that is required to support the INTOR concept.

The work was carried out by teams of experts working in their home institutions under the guidance of national INTOR participants. The INTOR participants from the four parties met periodically in Vienna

to review the work, make decisions, plan future work, and document the work of the workshop.

The INTOR activity was carried out in phases. At the end of each phase, the participating governments reviewed the progress of the activity and decided on the objectives of the next phase.

Phase 0 of the INTOR Workshop, which was conducted during 1979, addressed the first two objectives. Each partner submitted detailed contributions to the Phase 0 Workshop, which were subsequently published.<sup>1</sup> These contributions underwent extensive discussions at the workshop sessions and formed the basis for the Phase 0 Workshop report.<sup>1</sup> This report, which represents a technical consensus of the worldwide magnetic fusion community, concluded that the operation by the early 1990s of an ignited, deuterium-tritium-burning tokamak experiment that could serve as an engineering test facility was technically feasible, provided that the supporting R&D activity was expanded immediately, as discussed in the report. This broad international consensus on the readiness of magnetic fusion to take such a major step was in itself an important milestone in the development of fusion.

As a result of this positive conclusion, the INTOR Workshop was extended into Phase 1, the definition phase, in early 1980 on the basis of the IFRC review and recommendation to the IAEA. The objective of the Phase 1 Workshop was to develop a conceptual design of the INTOR experiment. The national conceptual design contributions to the Phase 1 INTOR Workshop form the basis for the INTOR conceptual design, which is documented in Ref. 2.

A number of critical technical issues were identified during Phase 1, with the potential for considerable improvements in the feasibility, cost, and engineering configuration of the INTOR design concept, if further work would lead to more advanced solutions than were available at the end of Phase 1. With this in mind, the INTOR Workshop was extended into Phase 2A, which was split off from Phase 2, detailed design of the experiment. In Phase 2A, emphasis was placed on resolution of the critical technical issues mentioned above. This work turned out to be fruitful and rewarding, but also time-consuming. As a consequence, Phase 2A was extended twice, so that there were finally three parts of Phase 2A: Part 1 from July 1981 to the end of 1982, Part 2 covering 1983 to mid-1985, and Part 3 covering mid-1985 to 1987.

Phase 2A, Part 1, concentrated on plasma performance, impurity control and the first wall, testing requirements, tritium and the blanket, mechanical configuration, magnetics and electromagnetics, and cost-risk-benefit. The work in the Phase 2A, Part 1, INTOR Workshop is reported in Ref. 3.

Phase 2A, Part 2, concentrated on impurity control, plasma heating and current drive, transient electromagnetics, maintainability, and technical benefit of partitioning INTOR component design and fabrica-

tion. A reassessment of the scientific and technical data base supporting the INTOR concept was also undertaken. As a consequence of these studies, some of the major parameters of the INTOR design concept were modified. The work of the Phase 2A, Part 2, Workshop is reported in Ref. 4.

Phase 2A, Part 3, began with the following intentions:

1. to address the following critical issues: impurity control, beta and confinement, heating and current drive, electromagnetics, configuration and maintenance, and the first wall and blanket
2. to reassess the demonstration reactor (DEMO) requirements
3. to study potential innovations that are not yet supported by developed physics or technology but could lead to improvement of the tokamak concept
4. to incorporate the results of all the work done during Parts 1, 2, and 3 of Phase 2A in an updating of the INTOR conceptual design.

During the course of Part 3, high-level discussions were held on another international collaborative activity, the joint design and construction of a next-step facility with aims similar to those of INTOR. The work orientation of the INTOR Workshop was reviewed, and it was decided to concentrate on critical issues, DEMO requirements, and innovations because these items are of immediate relevance to near-term tokamak design activities. Rather than updating only the INTOR conceptual design, a short, cumulative list of the results of this work was used for a critical analysis of all existing INTOR-like designs.

This work was carried forward in the usual manner, i.e., by teams of experts working in their home institutions under the direction of the INTOR participants, who met in Vienna five times (for a total of ~10 weeks) over the 2 yr of Phase 2A, Part 3, to define and review the work and to make decisions. This work was supported and/or prepared by INTOR-related specialists' meetings on impurity control, innovations, DEMO requirements, current drive, confinement, disruptions, and comparison of INTOR-like designs.

This paper summarizes the work of Phase 2A, Part 3, on critical issues, innovations, and data base assessment (Sec. II) and the analysis of INTOR-like designs (Sec. III). Implications for the INTOR design concept are discussed in Sec. IV. The objectives and parameters of the INTOR design concept have not changed during this phase and may be found in Ref. 4.

The detailed description of the U.S. contribution is the sixth and final U.S. INTOR report.<sup>5</sup> Previous U.S. reports are given in Refs. 6 through 10.

The cumulative INTOR work to date is a major factor in laying the groundwork for the design of the

next major experiment in the world tokamak program. Its objectives and general characteristics were defined. A preliminary conceptual design was developed early in the INTOR process and used to identify critical technical issues and R&D requirements. The critical technical issues have been partly resolved and elucidated by studies. The reactor design methods used by the four parties have been further developed and compared to test consistency. The national designs and the physical and technical constraints on which they are based have been evaluated. Finally, ways in which the INTOR design concept could be updated, based on this work, have been identified.

## II. CRITICAL ISSUES, INNOVATIONS, AND DATA BASE

Three of the critical issues of Phase 2A, Part 2, of the INTOR Workshop<sup>4,10</sup> were continued into Part 3 because considerable progress was expected from further work. These were impurity control, current drive and heating (with emphasis moving toward current drive), and electromagnetics. New critical issues were operational limits and confinement, and configuration and maintenance, the latter topic aiming at a critical comparison of different maintenance approaches. The blanket and first wall, the sixth critical issue, were reconsidered because it was expected that new information could lead to an updating of earlier conclusions.

During this phase, the INTOR Workshop was also charged with an analysis of proposed innovations to improve the tokamak concept. A collection of proposals and a first analysis were made during an INTOR-related specialists' meeting. The proposed innovations that looked promising and of sufficient impact were then considered by the relevant INTOR groups.

### II.A. Impurity Control

During Phase 2A, Part 3, work on impurity control was directed toward (a) updating previous assessments of experimental data for impurity control; (b) evaluating the potential relevance to INTOR of a number of innovative concepts; and (c) improving the consistency of plasma-edge modeling, with particular emphasis on model validation and improved prediction of divertor performance in INTOR-like tokamak reactors.

#### II.A.1. Experimental Data

There have been substantial new data from both poloidal divertor and limiter experiments in tokamaks. There is further new evidence that a divertor with an open geometry, of the type envisaged for INTOR, is capable of producing the high-recycling conditions that are necessary to minimize sputtering erosion of the divertor target. The concentration of impurities in the

main plasma is generally lower for divertor experiments than for limiter experiments (except for the H mode). However, the concentrations of low-Z impurities (e.g., oxygen) are not affected by a divertor as much as the level of high-Z impurities. There is often substantial emission of radiation within the divertor region, which is indicative of high-recycling conditions. It appears that H-mode operation can be obtained most easily with a poloidal divertor. In contrast, H-mode operation has been observed in only one limiter experiment. A disadvantage of the H mode is that, under certain conditions, it is accompanied by the accumulation of impurities on the plasma axis. Nonetheless, the temperature of the plasma that is in contact with the limiter during operation is high. This is likely to lead to high rates of sputtering and erosion of the limiter. Experiments on Tokamak Experiment for Technology Oriented Research (TEXTOR) indicate that exhaust of neutral gas can be quite efficiently performed by a pumped limiter.

#### II.A.2. Innovative Impurity Control Schemes

Five innovative schemes for impurity control in INTOR have been considered:

1. flow reversal of impurities as a consequence of coinjection of neutral beams
2. formation of a stable radiative edge at the periphery of the plasma column
3. an ergodic edge layer
4. burial of helium in the divertor region
5. liquid divertor plates.

The first three are not yet sufficiently well developed to be considered as candidates for the INTOR impurity control system. The last two show promise, and further theoretical and experimental work, together with the appropriate design analyses, is strongly encouraged.

#### II.A.3. Plasma-Edge Modeling

Improvements have been made in the two-dimensional numerical models used both for interpretation and prediction of plasma-edge performance. Comparison of the edge conditions calculated using the models with the conditions observed in experiments has enhanced confidence in such modeling. These models were used to analyze the projected performance of the INTOR divertor.

The conclusion of this work is that a high-recycling divertor with a tungsten target is the best available impurity control system to maintain a clean main plasma in INTOR and to ensure low target erosion during a fully inductive operational scenario. However, there are large uncertainties in plasma transport and in confinement requirements, and further R&D

and continuous reassessment of the expected performance of the present INTOR impurity control system are needed. Impurity control with current drive during an ignited burn is potentially different due to the increased power loads. A stable radiating edge layer and, in this respect, flow reversal would be beneficial. During inductive rampup, it is expected that adequate levels of high recycling can be established within the divertor. However, this is less certain in the case of noninductive rampup. Consideration has been given to the use of low- $Z$  target material (e.g., carbon and beryllium). Such materials are unlikely to be suitable for the more extended technology phase unless the divertor target surface can be readily renewed.

Improved modeling of impurity transport indicates that the pumping requirements for exhaust of helium ash may be more demanding than those specified in Phase 2A, Parts 1 and 2, i.e.,  $\sim 2 \times 10^5$  l/s of helium. Analysis of the innovative scheme for burial of helium in a continuously recoated metal layer within the divertor chamber indicates that it could be a useful adjunct to vacuum pumps.

Recent modeling confirms the previous prediction that divertor action provides efficient screening of the main plasma from impurities present in the edge. However, many uncertainties remain (e.g., cross-field transport of impurity ions, sputtering by superthermal ions, etc.) and continuing experimental and theoretical studies are required.

An overall conclusion from Phase 2A, Part 3, is that the poloidal divertor will, for INTOR, offer many advantages over a pumped limiter. Nevertheless, certain aspects of impurity control are presently uncertain, and both the conceptual design and the operational scenario for INTOR should be flexible in these particular respects.

## II.B. Current Drive and Heating

Several advances have recently been made in understanding auxiliary heating and noninductive current generation (NCG). These theoretical and experimental achievements confirm the benefits of several new techniques and give the designers more latitude in conceiving a device with operational flexibility.

### II.B.1. Experimental Results and Implications

In auxiliary heating, one particular accomplishment has been the testing of ion Bernstein wave heating (IBWH) on Princeton Large Torus<sup>11</sup> (PLT). A direct comparison with fast-wave minority (<sup>3</sup>He) heating on PLT showed nearly identical results for heating efficiency,  $\bar{n}_e \Delta T_{i0} / P_{rf} = 6.7 \times 10^{19}$  keV  $\cdot$  m<sup>-3</sup> / MW, with up to 650 kW of applied power. It is particularly noteworthy that IBWH results in very small ion tails, as the wave couples directly with the bulk ions. It is possible that this could result in favorable energy con-

finement for the ions, which remain nearly Maxwellian. The launching structure for IBWH is attractive for a reactor; unlike a fast-wave antenna, this launcher could be a pair of simple rectangular waveguides that, for frequencies  $\sim 130$  MHz, would require a vertical opening of  $\sim 1$  m and a horizontal width of  $\sim 2 \times 20$  cm through the first wall.

In contrast to IBWH, most other proposed auxiliary heating methods could also serve for NCG. The techniques most attractive for INTOR are neutral beam (NBCD), lower hybrid (LHCD), and fast-wave (FWCD) current drive. These systems offer adequately high electric-to-driver power efficiency ( $\geq 50\%$ ) and acceptable cost levels such that they can be considered for bulk current drive at power levels approaching 100 MW. The theory of NCG has matured in recent years with the inclusion of realistic effects, such as magnetic trapping, relativistic electron behavior, arbitrary ion charge, nonzero electric fields, Pfirsch-Schluter and bootstrap currents, and, for wave-driven currents, allowing for arbitrary wave polarizations, frequencies, and phase speeds. Most importantly for INTOR, high-power experiments with NCG are bearing out many of the theoretical predictions.

With regard to neutral beam injection (NBI), we note that NBCD on Tokamak Fusion Test Reactor<sup>12</sup> (TFTR) has maintained a current of 1 MA at densities  $> 1 \times 10^{19}$  m<sup>-3</sup> for 2 s with 6.0 MW of coinjection and 4.6 MW of counterinjection. Experimental evidence of NBCD has invariably been in good agreement with theoretical predictions, so we feel that NBCD would be a reliable option for high-density operation of INTOR. However, to achieve a centrally peaked current density profile, it will be necessary to inject at energies  $\geq 1$  MeV. This is a difficult challenge that requires a period of negative ion source and accelerator development. Additionally, there is concern that such high beam energies may drive an Alfvén wave instability in the plasma, resulting in a possibly degraded NBCD efficiency.

At low densities, the LHCD option appears to be complementary to the neutral beam. Experiments have shown impressive results at low densities: On JT-60, a current of 2 MA is maintained at  $\bar{n}_e = 3 \times 10^{18}$  m<sup>-3</sup> for 2.5 s with 3.0 MW of power.<sup>13</sup> The efficiency, defined as  $\gamma = \bar{n}_e IR / P$  (10<sup>20</sup> A  $\cdot$  W<sup>-1</sup>  $\cdot$  m<sup>-2</sup>), is theoretically an increasing function of electron temperature  $\bar{T}_e$ , and this result is evident from tokamak experiments spanning a wide range of  $\bar{T}_e$  values. The PLT reports  $\gamma = 0.15$ , and JT-60 doubles this figure of merit (FOM) to  $\gamma = 0.30$  when additional intense plasma heating is employed. Theoretical limitations to LHCD may restrict its use, however, to the low-density and low-temperature surface region of INTOR during full-power operation.

On the other hand, good wave penetration and central current generation are possible with LHCD at very low density ( $< 10^{19}$  m<sup>-3</sup>) on INTOR, which would

permit current rampup prior to burn or quasi-steady-state operation with periodic transformer recharging at low density between burns.<sup>14</sup> This LHCD option during low-density transients implies the simultaneous presence of electric fields that drive additional Spitzer currents. The theory of LHCD combined with electric fields has been developed,<sup>15</sup> and data analysis shows that the relevant experiments on PLT, Axially Symmetric Divertor Experiment (ASDEX), and Alcator C are in good agreement with expectations.<sup>16</sup> Likewise, JT-60 has shown partial transformer recharge while maintaining ~1 MA of toroidal current.

II.B.2. Current Drive Efficiencies for INTOR

Encouraged by the good agreement between theory and experiment, it was decided to calculate the expected current drive performance for INTOR. A series of calculation tasks were defined, and all four INTOR participants were requested to carry out the analyses using their best national computation codes for a benchmark comparison. Four driver candidates were considered for this study: NBCD, LHCD, and FWCD at both high frequency (approximately gigahertz) and low frequency [ion cyclotron resonance frequency (ICRF)].

The first task was to compute the efficiency  $\gamma$  for steady-state NCG at  $\bar{n}_e = 7 \times 10^{19} \text{ m}^{-3}$  and  $\bar{T}_e =$

20 keV, requiring a centrally peaked current density and setting the electric field to zero.

For NBCD, an impurity content with  $Z_{eff} = 2.0$  was specified, and  $\gamma = 0.37$  was found by the United States, with a deuteron energy  $E_b = 0.75 \text{ MeV}$ . This agrees very closely with the value obtained by most other INTOR participants (see Table I). A sensitivity study was done to infer the temperature dependence of  $\gamma$  for NBCD. For a fixed beam energy, we found  $\gamma$  increases with  $\bar{T}_e$ , our results coinciding with the Japanese scaling,  $\gamma \cong 0.064 (\bar{T}_e/\text{keV})^{0.58}$ . The variation of  $\gamma$  with  $Z_{eff}$  is quite flat in the  $1.5 \leq Z_{eff} \leq 3.0$  range. We find  $\gamma$  has a maximum for  $E_b \geq 1.0 \text{ MeV}$ , and  $\gamma$  significantly deteriorates for  $E_b \leq 0.5 \text{ MeV}$ .

For LHCD, it was not possible to generate a centrally peaked current density for the specified steady-state INTOR plasma, due to the strong wave damping, which prevents penetration beyond  $T_e \geq 10 \text{ keV}$ .

In contrast to LHCD, the fast wave may be accessible to the interior region of the INTOR plasma. In our work with high-frequency FWCD (Ref. 17), we chose a number of sources with frequencies from 0.3 to 1.0 GHz, and we tailored the power spectrum ( $1.6 \leq n_{||} \leq 2.8$ ) to achieve a self-consistent magneto-hydrodynamic (MHD) equilibrium with 3.62% beta and a smooth safety factor ( $q_{axis} = 1.01, q_{edge} = 2.37$ ); the calculation was done with a noncircular cross section (elongation of 1.6) and for an aspect

TABLE I  
Benchmark Steady State  $\gamma$  ( $10^{20} \text{ A} \cdot \text{W}^{-1} \cdot \text{m}^{-2}$ )  
Values for  $\bar{T}_e = 20 \text{ keV}$ ,  $\bar{n}_e = 0.7 \times 10^{20} \text{ m}^{-3}$ ,  $E = 0$

Driver	European Communities	Japan	United States	USSR
LHCD $f = 2 \text{ to } 10 \text{ GHz}$ $1.7 \leq n_{  } \leq 4.0$ $Z = 1.5$	(0.5) <sup>a</sup>	(0.3) <sup>a</sup>	(0.3) <sup>a</sup>	(0.5 to 0.8) <sup>a</sup>
NBCD $0.4 \text{ MeV} \leq E_b \leq 0.7 \text{ MeV}$	0.39	0.37	0.37	0.5
High-frequency FWCD $f = 0.3 \text{ to } 1.0 \text{ GHz}$ $1.4 \leq n_{  } \leq 2.8$ $Z \cong 1.5$	---	0.3, <sup>b</sup> ray tracing 0.6, <sup>c</sup> full wave	0.41	0.31 <sup>c,d</sup>
Low-frequency FWCD $f = 22 \text{ to } 70 \text{ MHz}$ $3.0 \leq n_{  } \leq 4.5$ $Z \cong 1.5$ , transit time magnetic pumping	---	(0.08) <sup>d,f</sup>	0.33	0.27 <sup>d</sup>

<sup>a</sup>Centrally peaked current density not found at  $\bar{T}_e = 20 \text{ keV}$  if accessibility or frequency constraint is imposed.

<sup>b</sup>Single-pass result multiplied by  $P^{in}/P^e = (0.6)^{-1}$ , assuming multipass absorption.

<sup>c</sup>Scaled by value at 15 keV by  $(20/15)^{0.34}$ .

<sup>d</sup>Includes factor of 2.0 to account for two-dimensional velocity space.

<sup>e</sup>Includes factor of 2.5 to account for two-dimensional velocity space.

<sup>f</sup>Calculated at  $\bar{T}_e = 5 \text{ keV}$ ; uses  $n_{||} = 12$ .

ratio of 4.2. The result with  $Z_{eff} = 1.5$  and  $\gamma = 0.41$  is within the range of values found by other INTOR participants (see Table I). At this beta value, we find the temperature scaling is  $\gamma \cong 0.041 (\bar{T}_e/\text{keV})^{0.77}$ . In the  $1.0 \leq Z_{eff} \leq 2.0$  range, we find  $\gamma \propto Z_{eff}^{-0.373}$ . These sanguine findings for FWCD must be tempered with the knowledge that experimental evidence for FWCD is sparse, and there is concern, especially at high frequencies, that the fast wave may anomalously couple to the slow wave and suffer the same poor penetration experienced for high-density LHCD.

On the other hand, at low frequencies the fast wave is well known from ion cyclotron resonance heating (ICRH) experiments to penetrate easily to the magnetic axis. The FWCD calculations at these frequencies have not yet been refined, but, in agreement with the other INTOR participants, we find that centrally peaked current profiles are possible: For  $Z_{eff} = 1.5$ , we compute  $\gamma = 0.33$ . For this calculation, the 64-MHz frequency was chosen such that wave damping and FWCD are achieved by transit time electron pumping near the axis; only  $\sim 10\%$  of the wave power is lost to second-harmonic tritium cyclotron damping. Our ray-tracing result is in rough agreement with the full-wave calculation done by the USSR (see Table I).

### II.B.3. Control of Current Density Profile

The second task assigned to the four national teams was to assess the possibility of controlling the current density profile by manipulating the parameters for the four candidate NCG methods. This exercise was motivated by observations that NCG can result in tokamak experimental operation with MHD properties differing from conventional ohmic performance.<sup>18</sup> Decoupling the current density and temperature profiles may eliminate sawteeth and perhaps permit operation at higher beta than is possible in the usual Troyon regime experienced with ohmic current generation. Both NBCD and FWCD were shown to allow current profile control. For NBCD, the best control was achieved by varying the height of the rectangular beam cross section; broad or even hollow profiles are achieved with substantial injection into the relatively low-density plasma well above and below the midplane, while more centrally peaked profiles result from injection concentrated near the midplane. The high-frequency FWCD method provides the best profile control seen in our calculations. By launching a power spectrum rich in low- $n_{\parallel}$  components, centrally peaked currents were found. By shifting power to high  $n_{\parallel}$ , hollow currents can be created. One example is in MHD equilibrium with a monotonic (single-value) safety factor and a beta over twice the Troyon value. Indeed, FWCD should allow operation with  $q_{axis}$  well above unity, possibly permitting operation in the second stability regime.

Studies of profile control with FWCD in the ICRF

have not yet been done. On the other hand, LHCD is presently felt to have little control flexibility because it may be suited only for low-density plasma regions. Hence, LHCD would necessarily be combined with some other driver if it were to be useful in this context.

### II.B.4. Current Drive Power Requirements

The final task, which compared only LHCD and NBCD, was to calculate the power required to maintain 8 MA of current with a reverse electric field,  $E = -0.01$  V/m, assuming low density and temperature, as would occur during noninductive current rampup or transformer recharge. We find LHCD is well suited for this purpose. With  $\bar{n}_e = 4 \times 10^{18} \text{ m}^{-3}$ ,  $\bar{T}_e = 2$  keV, and  $Z_{eff} = 1.5$ , we find that a centrally peaked profile can be held in equilibrium with 24 MW of power. Our result, which is somewhat pessimistic compared to the European Communities and USSR values (14 and  $\sim 20$  MW, respectively), seems to be quite acceptable for an INTOR-sized tokamak. In contrast, NBCD for this application is less attractive. To avoid excessive shinethrough at  $E_b \cong 0.5$  MeV, it may be necessary to maintain a higher density,  $\bar{n}_e \cong 6 \times 10^{18} \text{ m}^{-3}$ . Power balance considerations suggest  $\bar{T}_e \cong 6$  keV with NBCD under these conditions, and we find 34 MW is needed ( $Z_{eff} = 9$ ). Japan and the USSR are less optimistic on this issue, predicting 47 and 40 MW, respectively, under similar conditions (but,  $\bar{n}_e = 8 \times 10^{18} \text{ m}^{-3}$ ).

### II.B.5. Bootstrap Current

In a separate study, we also considered the benefits of the neoclassical bootstrap current for reducing NCG power. According to theory, a small seed current must be provided near the magnetic axis (e.g., by NBCD or FWCD), and the bootstrap current will then appear over the bulk plasma when the tokamak is in the banana regime. We calculated the FWCD efficiency  $\gamma$  without bootstrap contributions and the efficiency  $\gamma_B$  including bootstrap currents for identical MHD equilibria, and we studied the dependence of  $\Gamma \equiv 1 - (\gamma/\gamma_B)$  on tokamak parameters for a large variety of equilibria. Because we have  $\gamma_B = \bar{n}_e IR/P_B$ , where  $P_B$  is the (smaller) driver power required to achieve equilibrium with the aid of the bootstrap effect, we see  $\gamma_B > \gamma$ ; and  $\Gamma$ , which is the fractional reduction of driver power, will approach unity as the bootstrap effect predominates. If we define a peak poloidal beta  $\beta_{10} = 2 \mu p_0 / \langle B_p \rangle^2$ , we can fit our extensive calculations by

$$\Gamma \cong \begin{cases} C\beta_{10}/(4\sqrt{A}) , & C\beta_{10}/\sqrt{A} \leq 3.6 \\ 0.9 , & C\beta_{10}/\sqrt{A} > 3.6 \end{cases}$$

The coefficient  $C$  is a function of  $Z_{eff}$ , peak density and temperature, and the plasma profiles. (Details of this work will be published separately.) For INTOR with congruent profiles ( $d \ln T/d \ln n = 1$ ), we find



$\Gamma \geq 0.9$  at high density ( $\bar{n}_e = 1.4 \times 10^{20} \text{ m}^{-3}$ ), which requires FWCD with only  $P \cong 10 \text{ MW}$ . While this very modest amount of external power would make steady-state operation quite attractive, we caution that flatter density profiles will significantly reduce  $\Gamma$ . By varying the density and temperature profiles, we found that  $\Gamma \leq 0.5$  would be likely for flatter density profiles. Note that the bootstrap current may be particularly relevant to steady-state INTOR operation in light of the positive experimental results seen on TFTR (Ref. 12).

## II.C. Operational Limits and Confinement

Operational limits to stable tokamak operation, disruptions, and the confinement properties of tokamak plasmas are key issues for INTOR. In these areas, an updating of the data base has been undertaken and innovative ideas have been analyzed, in particular with respect to enhancing the beta limit. A specific effort was dedicated to advancing the ideal MHD stability analysis beyond the limits explored in the past.

### II.C.1. Beta Limit

Experimental results on the operational limit to the plasma beta correspond to values of the Troyon  $g$  factor in the 3 to 3.5%  $\cdot \text{T} \cdot \text{m}/\text{MA}$  range, provided that  $q_a$  is above a critical value that increases with decreasing  $A$ . A normal conductor toroidal field (TF) coil set would be required to economically use such high beta values. For indented plasmas, while the ideal ballooning stability limit is enhanced, the kink mode is destabilized so that efficient wall stabilization is essential for achieving high beta. It remains uncertain whether this can be provided. The second stability regime of ideal ballooning modes can be reached either in D-shaped plasmas for sufficiently high  $q_0$  or in sufficiently indented plasmas. However, in these cases, kink-mode instability is enhanced. Furthermore, a wide range of the plasma has to be nearly shear-free, a situation in which low- $n$  internal modes tend to be destabilized. Resistive destabilization of high- $n$  modes is also a concern. In conclusion, moderately elongated D shapes ( $K \approx 2$ ) appear attractive for INTOR and allow enhancement of the plasma beta. Unconventional solutions to increase beta are too uncertain to rely on at the present time.

### II.C.2. Density Limit

The density limit, if extrapolated according to common Murakami-Hugill-like scalings, tends to be a more stringent limitation to the plasma pressure than the beta limit at temperatures  $T \leq 10 \text{ keV}$ . However, the physics understanding of this limit is incomplete, and results for discharges with intense additional heating generally show an enhancement of the density limit and indicate large deviations from the Murakami-Hugill scaling. In Joint European Torus (JET), the

density limit appears when the radiation losses become equal to the power input, a criterion that, when extrapolated to INTOR, predicts an appreciably higher density limit than the Murakami-Hugill scaling. Quantitative predictions, however, sensitively depend on the plasma-edge parameters in this case. The limit to the safety factor, at least at modest values of beta and for conventional circular and D-shaped plasmas, is  $>2$  (at 95% of the magnetic flux for poloidal divertor configurations). This limit is seen to increase to  $>3$  as the beta limit is approached or when the elongation is increased beyond 2.

### II.C.3. Disruptions

Operational limits are often due to the appearance of disruptions. The available data base on major disruptions was analyzed and the disruption specification for INTOR was updated. In view of results from JET and TFTR, very short energy quench times, of the order of 0.1 ms, must be considered to be a possibility in INTOR. The energy deposition profile in a poloidal divertor configuration remains unknown, so deposition of up to the total plasma kinetic energy on either the divertor plates or the first wall must be considered. The current quench rate is determined by the evolution of the plasma parameters after energy quench, taking account of the electromagnetic coupling to the surrounding passive conducting structures and the capacity of the active position control device. If efficient position control is provided, a maximum current decay rate of  $3 \times 10^8 \text{ A/s}$  appears appropriate for INTOR.

### II.C.4. Confinement

Extrapolation of plasma confinement to INTOR conditions still contains large uncertainties (by more than one order of magnitude). Operating INTOR in a regime of improved confinement (H mode) is considered reasonable, although major uncertainties remain with respect to the reactor relevance of this regime. These uncertainties are related to the existence of controlled steady-state operation with low impurities, to its compatibility with radio-frequency heating and current drive, and to efficient power and particle exhaust under acceptable divertor plate and first-wall working conditions. Also, the scaling of energy confinement in the H mode remains uncertain, particularly with respect to plasma size, plasma temperature, heating power, and, to some extent, plasma current and density. These are key research issues in the ongoing tokamak physics program and are expected to be clarified before the construction of INTOR-like devices.

### II.C.5. Fast Alpha-Particle Loss

The fast alpha-particle losses due to TF ripples resulting from ripple trapping and ripple-induced diffusion of banana orbits (stochastic diffusion) were

studied. For ripple values around 1% (peak to average), the latter is the dominant mechanism. It is estimated that for INTOR, ~2 to 3% of the fusion alpha energy and ~4 to 7% of the fusion alpha particles are lost through this mechanism. It is shown that the alpha-particle flux to the wall is localized between the TF coils and displaced from the midplane at small poloidal angles. However, these results are different from those produced at Japan Atomic Energy Research Institute recently, which indicated losses more than three times the above values.

Comparison of the models and the numerical procedures used in these computations has identified apparently important differences. These include differences in the numerical integration approaches, in the approximations of the scattering operator of the charge particles, and in the presence of an artificial speedup of the time scale of integration. Work is needed to resolve these discrepancies and to test the results in experiments.

## II.D. Electromagnetics

### II.D.1. Poloidal Field System Optimization

To design poloidal field (PF) coil systems that are consistent with a chosen plasma configuration, it is desirable to identify coil locations that minimize the PF energy. Several optimization codes exist that can solve this generalized free-boundary Grad-Shafranov equilibrium problem. However, at several of the past INTOR workshops, discrepancies have been noted between INTOR delegation predictions for the coil currents necessary to produce a given plasma configuration. To understand the source of the discrepancies, some benchmark equilibrium calculations were performed. The plasma shape, current profile, and beta were precisely defined, and the positions of the PF coils were given. Minimum-energy PF coil currents were sought that produced the specified equilibrium configuration (the actual plasma boundary being fit to the desired shape in a least-squares sense). When results were compared with the various delegations, good agreement was consistently found, giving confidence in the validity of the computer codes. The previously obtained discrepancy in results is understood to be due largely to the sensitivity of the required PF coil currents to the assumed plasma beta and plasma current profile. The beta dependence arises because although the primary role of the outer PF coil nearest the midplane is to provide the vertical field for radial equilibrium, this coil also provides significant volt-seconds. The higher the beta, the more volt-seconds are provided; therefore, calculations performed at fixed volt-seconds give rise to different PF coil currents when beta is varied. It is also found that the dependence of required coil current on plasma current profile can be sensitive. Simulations performed for an early Compact Ignition Tokamak (CIT) design (major

radius 1.75 m, minor radius 0.55 m, plasma current 9.0 MA), for example, indicate that varying the plasma  $li/2$  from 0.30 to 0.50 can change the location of the null point by several centimetres. Calculations that constrain the shape to be constant must compensate for this change by adjusting the coil currents appropriately.

The PF coil system for the baseline single-null INTOR configuration has been optimized relative to the ohmic heating (OH) flux swing bias at start-up and at end-of-burn by studying the sensitivity of selected PF design variables (stored energy, ampere-metres, coil current density, and maximum magnetic field) to chosen biases. The central solenoid current density and maximum field levels are the most strongly dependent variables, and they set the optimum swing from +46 to -66 V·s for a total of 112 V·s provided.

### II.D.2. Impact of Maintenance Scheme

The impact of maintenance scheme (horizontal versus vertical access) on the PF configuration and magnetic energy was considered. A highly elongated plasma requires a vertical field (VF) with a curvature such that the field index is negative. The most natural location for a VF coil is therefore near the equatorial plane. If the primary VF coil has to be placed at some distance  $\Delta z_{coil}$  from the midplane, the vertical field seen by the plasma is weighted by the cosine of the angle between the equatorial plane and the line from the plasma to the coil. As  $\Delta z_{coil}$  increases, the coil current must increase to give the same vertical field. Moreover, the same coil now contributes some higher order multipole (shaping) component, which can interfere with the shaping component of the main divertor coil. Both of these effects tend to increase the magnetic field energy and total megampere-metres, which are found to be sensitive functions of  $\Delta z_{coil}$ . No matter what maintenance scheme is chosen, the existence of an auxiliary heating port imposes an exclusion zone for the placement of PF coils close to the midplane. The actual size of this zone depends on design details. In a vertical maintenance scheme, the size of the heating port is the main determinant of the outboard exclusion zone, whereas, in a horizontal maintenance scheme, the outboard exclusion zone can be expected to be larger. Since the PF energy depends sensitively on  $\Delta z_{coil}$ , it is not possible to argue strongly in favor of one scheme over another, because minor changes in the assumptions of the size of the exclusion zone can alter the conclusion. As a general principle, it is advantageous to minimize  $\Delta z_{coil}$ .

### II.D.3. Disruption Electromagnetic Modeling

Considerable progress has been made in the development and benchmarking of the Tokamak Simulation Code (TSC). This free-boundary axisymmetric simulation code was developed to model the transport



time scale evolution and the positional stability and control properties of noncircular tokamaks. The validity of TSC has been tested against various analytical plasma models, but, more importantly, it has been validated by comparison of code predictions with controlled experimental shots from the Princeton Beta Experiment, TFTR, and DIII-D. The code has also been used to simulate the plasma behavior during a major disruption on TFTR where current quench decay rates of  $\sim 1$  MA/ms were experimentally observed. Code developments include (a) the implementation of an improved feedback capability allowing realistic modeling of most tokamak control systems; (b) the capability of modeling a time-varying toroidal magnetic field, allowing it to be simultaneously ramped with the toroidal current; and (c) the inclusion of alpha-particle heating terms in the transport section of the code, which allows the modeling of ignition experiments. The TSC has been used to model the current ramp and burn phases of the proposed CIT experiment and has been useful for examining the volt-second requirements.

The results of simple models for predicting wall loads during major plasma disruptions show that results can be very sensitive to the assumptions regarding the action of the plasma during a disruption. Typically, in the simple models, the plasma current is assumed to ramp linearly to zero in a given time, at a fixed location, or else the plasma is forced to move along some predetermined trajectory while the current is quenched. The sensitivity of the results to the assumptions shows the need for codes that treat the plasma and its interaction with external magnetic fields in a more consistent way. The TSC has been used to simulate several disruptions on TFTR and DIII-D. Because the code incorporates a detailed transport model, the thermal quench phase of the disruption can be simulated, as well as the subsequent current quench. When model parameters are chosen appropriately, the results of TSC have been shown to agree well with the experiments. The DSTAR computer code developed at the Idaho National Engineering Laboratory couples TSC with other packages that quantify the surface erosion and induced forces that occur during major plasma disruptions. The DSTAR code has been used to predict current quench rates and thermal and mechanical loads in the first wall, blanket, and shielding (FWBS) for INTOR. The rates are found to be sensitive to the disruption scenario, and they can be particularly high if the internal disruption follows a vertical instability because of contamination of the plasma from impurities when the disruption occurs while the plasma is near the divertor plate. The predicted current quench rates can be as high as 3 MA/ms. There are uncertainties in the modeling parameters used to simulate the disruptions, but it is believed likely that current quench rates well in excess of 1 MA/ms will occur.

#### *II.D.4. Operating Scenarios*

Operating scenarios for INTOR have considered the use of separate control coils to provide active vertical stabilization of the plasma. A rapid vertical plasma displacement would be initially restrained by fields due to eddy currents induced in passive conducting structures; then the active coils would be excited to provide the required stabilization field. By using a static plasma model with a variable current density, "contours of constant effectiveness" of passive material can be traced, which indicate where the placement of conducting material is most effective in stabilizing the vertical motion of the plasma on the ideal time scale. When the location of these contours is compared with an outline of the INTOR baseline design, it is found that the most effective material is on the outboard side. Although the bulk of the conducting material in the machine is ineffective, we have concluded that no additional passive coils need to be incorporated into the design. This result is in agreement with earlier results, which employed a more elementary treatment of the plasma as a single current filament.

#### *II.D.5. High-Field Superconducting Magnets*

The principal innovation recommended to the INTOR study is the incorporation of high current density, high-field superconducting magnets. When combined with improved radiation tolerance of the magnets to minimize the inner shielding of the tokamak, a substantial reduction in machine dimensions and capital costs can be achieved. Cable-in-conduit conductors (CICC) are capable of the desired enhancements and are under development. Because conductor stability in a CICC depends more on the enthalpy of the interstitial helium than the copper resistivity, high stability is retained at current densities of the order of 40 A/mm<sup>2</sup> and fields as high as 12 T, even with high heat loads. Radiation damage to the copper stabilizer is less important because the growth in resistance is a second-order effect on stability. Such CICC conductors lend themselves naturally to niobium-tin utilization, with the benefits of the high current-sharing temperature of this material being used to advantage in absorbing radiation heating. The constraints on current density imposed by protection criteria must still be met, but these are ameliorated by the selection of higher operating current (made feasible by a wind-and-react fabrication technique). In this way, it is possible to consider both higher fields and current densities for INTOR.

Peak nuclear heating rates  $>5$  mW/cm<sup>3</sup> are cryogenically acceptable with large refrigerators. This corresponds with neutron fluences of  $\sim 10^{19}$  n/cm<sup>2</sup> or insulator radiation doses of  $10^{10}$  rads in  $10^8$  s. These values are compatible with next-generation engineering test reactors if radiation-resistant polyimide insulators are used to provide the main voltage standoff.

The radial build out to the inner first wall, when

coupled with the physics requirements for good performance, sets the major radius of the tokamak. Minimizing the radial build by the use of higher current densities and allowing higher heat loads can be a major factor in reducing the size and hence cost of INTOR.

## II.E. Configuration and Maintenance

The critical issues and innovations dealing with configuration and maintenance consisted of six tasks.

### II.E.1. Vertical and Horizontal Access Configurations

The INTOR configuration is based on the horizontal removal of torus sectors, including the biological shield, for the replacement of first-wall/blanket components. The comparative study between this approach and the vertical approach is based on a configuration similar to the Next European Torus (NET), whereby first-wall/blanket components are removed in a vertical fashion. The primary difference between these con-

figurations is the location of the PF coils and the emphasis of the maintenance philosophy. The INTOR design was initially developed with simplified maintenance as the primary objective, i.e., straight, radial extraction of complete torus sectors. This led to a configuration where the PF coils were positioned to provide a large window opening for the sector without considering the impact on the cost of the PF system. The vertical access design, shown in Fig. 1 as a modification to the INTOR baseline, has PF coils located to provide a small horizontal window for heating and test modules and a vertical access port for removal of first-wall/blanket components.

A comparison of these approaches showed that the latter design had a 25% reduction in the cost of the PF coils; however, most of that reduction was the result of reducing the diameter of the lower outboard coil. The cost reduction from relocating the other coils was ~7%. This modest reduction is the result of a low plasma elongation of  $k = 1.6$ . Further study showed that for elongations  $\geq 2.0$ , PF cost reductions are substantial.

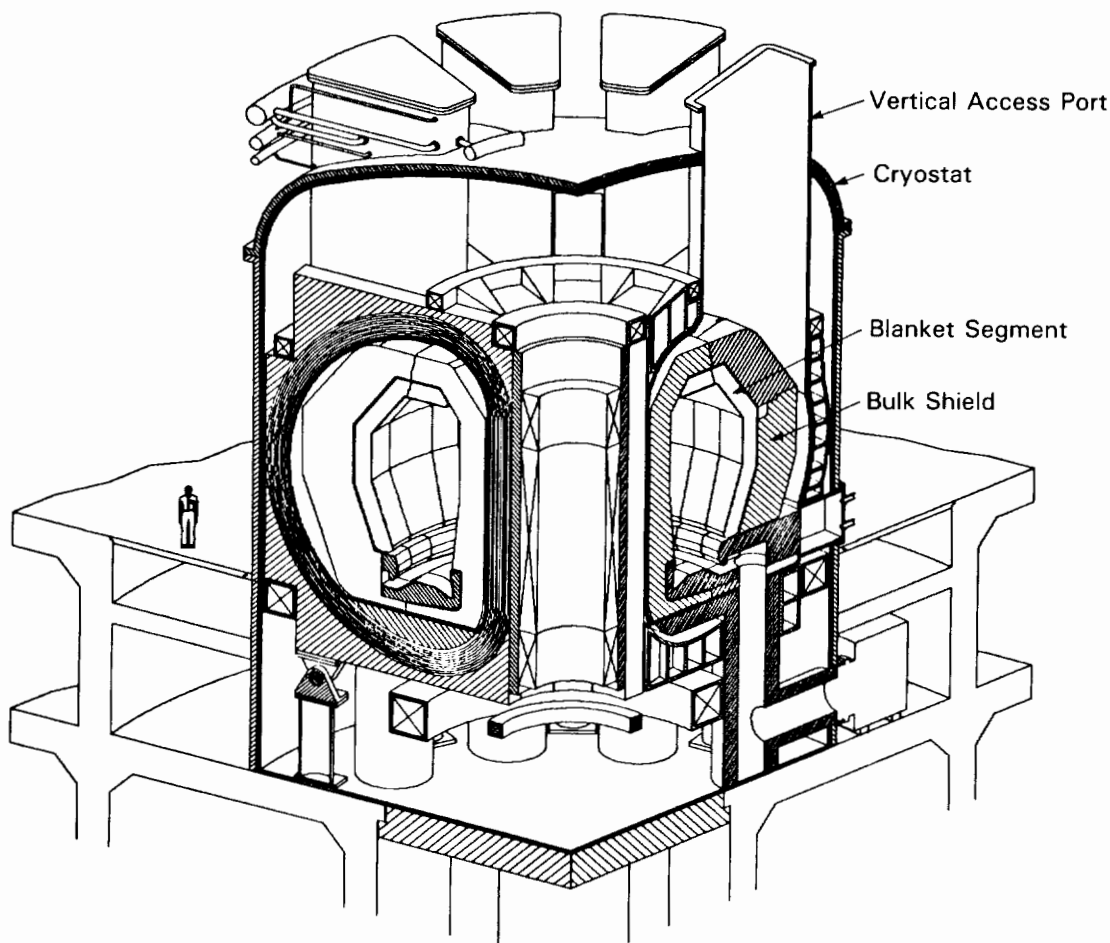


Fig. 1. INTOR concept based on vertical access for replacing first-wall/blanket components.

Time and motion studies for replacing first-wall/blanket components did not reveal any substantial difference in the maintenance time required. Both approaches were within 10% of each other for downtime. Also, it does appear possible to vertically remove internal reactor components without disturbing peripheral equipment, such as heating and test modules. While this is clearly an advantage, vertical removal requires more first-wall/blanket segments and complex handling equipment. The configuration shown in Fig. 1 has 48 blanket segments corresponding to 12 torus sectors. The greater number of segments requires a more complex arrangement of cooling pipes, and the greater number of surface gaps and mechanical connections will reduce the effective blanket surface available in the torus.

Based on the level of design detail to date, it appears that both approaches are feasible. For higher elongation plasmas, a vertical access approach with optimized PF coil locations should be pursued in conjunction with developing feasible segmented blanket designs.

### *II.E.2. Shape-Memory Alloys*

Shape-memory alloys (SMAs) are widely used for hydraulic pipe couplings and appear suitable for vacuum joints. These alloys are based on compounds of nickel and titanium and derive their shape-memory properties from austenite/martensite transformations, which are a function of temperature. Couplings made from these compounds are simpler and faster to make than alternatives such as welding. SMA applications for INTOR are proposed for cooling pipe connectors, mechanical quick connectors, and metal packing for vacuum seals.

The unique aspect for INTOR applications is the neutron environment. Results from tests in Japan using fast neutrons (0.1 MeV) at 323 K at a fluence of  $8 \times 10^{19}$  n/cm<sup>2</sup> presented no problems, indicating that SMA could be used outside the INTOR shield. Recent work at Oak Ridge National Laboratory using ion bombardment to predict the effects of fluence and temperature indicates that SMA may be used behind the blanket structure.

The use of SMAs will not affect the configuration, but they have the potential to reduce the downtime for certain maintenance operations. In particular, they are suited for unexpected repairs in areas with limited access.

### *II.E.3. Ferromagnetic Inserts*

Ferromagnetic inserts located in front of the TF coils effectively reduce the TF ripple. The magnetic flux produced by the inserts increases the field in the plasma region between coils and reduces the field in the plane of the coils. This reduction of field ripple

makes it possible to reduce either the number of TF coils or their size.

Analysis shows that it is possible to reduce the outer leg of the INTOR coils by 0.5 m radially. However, from a maintenance point of view, access to the torus is correspondingly reduced. On the other hand, a reduction in the number of coils from 12 to 10 results in a proportionate increase in midplane toroidal access. This can be achieved by incorporating the ferromagnetic material into the torus shield and, because the shield is already a substantial structure, reacting the electromagnetic forces should be manageable. These forces can be as high as 20 MN.

### *II.E.4. PF Coil Redundancy*

Untrapped PF coils are the basis of the PF system in the reference design. However, the cost penalty for the lower outboard coil weighing 600 tonnes is ~18% compared to a more natural position closer to the plasma under the TF coils. A failure of this coil in its optimized position requires a major disassembly of the reactor. Hence, it requires extreme reliability or built-in redundancy.

High reliability can be achieved by making the coil larger and operating it at reduced current density. Redundancy can be achieved by installing spare coil segments with independent leads and structure. In the first approach, present technology cannot guarantee faultless operation. For the second, the questions are the required number of segments and the amount of space that can be devoted to additional leads and structure.

An approach that appears satisfactory compared to the present baseline is to locate the lower outboard coil in its optimum position under the TF coils. In addition, during construction, provisions for the large trench (as in the baseline) should be incorporated into the reactor hall. In the event that this trapped coil should fail, it can be abandoned in place and a larger, less efficient coil can be installed in the trench as in the baseline. The impact to reactor downtime for coil replacement will be the same, because in the present baseline a spare coil has not been assumed. If the trapped coil does not fail, a substantial cost benefit results from the reduced PF system cost. The downtime to replace a lower outboard coil may approach 3 yr: 1 yr to procure material, 1 yr for winding and testing, and 6 months to 1 yr for coil installation and resumption of reactor operations.

### *II.E.5. Rapid Replacement for Divertor/First Wall*

Rapid replacement of these in-vessel components was based on maintaining the vacuum integrity of the plasma chamber. The present baseline requires a detritiation bakeout that has been estimated at 1 week

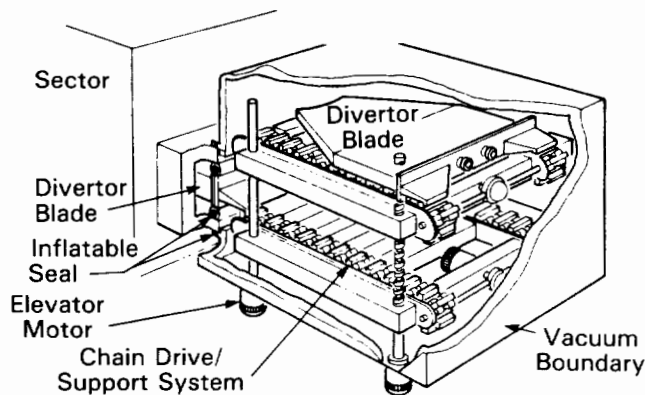


Fig. 2. Containment concept for remote replacement of a divertor module.

and a plasma chamber reconditioning also for 1 week. Therefore, if these components can be replaced under vacuum conditions, a significant saving in downtime is possible. Figure 2 shows a concept for remotely replacing divertors using this approach. The design incorporates isolation valves and a spare divertor module. Since the divertors are estimated to require annual replacement, the downtime savings will offset the cost of developing this equipment.

This is not the case for replacing torus sectors in evacuated structures. Each sector is  $\sim 4 \times 7 \times 5$  m; hence, the containment structure is an unreasonable size and will affect the reactor hall size. In addition, the INTOR first wall is considered to be a lifetime component; therefore, any replacements will be unscheduled and infrequent.

#### II.E.6. Containment of Tritium and Activated Dust

Bakeout for detritiation and in-vessel cleaning for the collection of solid particulates will be required before opening the plasma chamber. Reduction of secondary outgassing and activated dust can be accomplished by maintaining a slightly negative pressure in the torus with the use of the vacuum pumping system. Replacement of components such as test modules or divertors, using equipment like that shown in Fig. 2, automatically provides containment. Large components such as a torus sector may be extracted into shroudlike containments, although additional study for this approach is needed to determine if particulate afterheat will damage these flexible structures.

#### II.F. Blanket and First Wall

This phase of the blanket and first-wall study focused on four areas:

1. an update of critical materials data base for INTOR

2. first-wall design and performance analysis
3. development of blanket concepts capable of providing tritium self-sufficiency
4. materials and nuclear technology R&D.

##### II.F.1. New Materials Data Base

New materials data have been reviewed on austenitic and ferritic steels, graphite and carbon-carbon composites, ceramic breeder materials, liquid breeder materials, divertor materials, and magnet materials.

*II.F.1.a. Austenitic Steels.* Additional information on three critical issues for austenitic steels was presented: (a) the sensitivity to aqueous stress corrosion, (b) low-temperature radiation effects on mechanical properties, and (c) effect of radiation on weldments. Aqueous stress corrosion cracking of austenitic steels, particularly in the presence of irradiation, is identified as a serious feasibility issue for the reference INTOR first-wall/blanket structure. Significant loss of tensile ductility is also a major concern. Austenitic stainless steel is the only reasonable structural material for the low-temperature first wall and blanket of INTOR.

*II.F.1.b. Ferritic/Martensitic Steels.* The selection of ferritic/martensitic steel as the first-wall/blanket structure for the low-temperature, cyclic operating conditions of INTOR is not recommended. The ductile-to-brittle transition temperature (DBTT) of ferritic steels is increased more than  $200^\circ\text{C}$  by low-temperature ( $<300^\circ\text{C}$ ) irradiation. The effect of hydrogen is of particular concern at the low temperatures where release of the internally generated hydrogen may be inhibited. The hydrogen effect may be even more critical for irradiated material, e.g.,  $\Delta\text{DBTT}$ , and/or for weldments.

*II.F.1.c. Graphite and Carbon-Carbon Composites.* Three aspects of graphite and carbon-carbon composites, form of redeposited material, radiation effects, and tritium retention, have been evaluated. The effect of high helium generation rate (helium/dpa  $\sim 300$ ) is unknown but may be significant at low temperatures ( $<1200^\circ\text{C}$ ). The carbon-carbon composites provide significant tensile strength and fracture toughness; however, they are predicted to be significantly less resistant to radiation damage because of the large anisotropy of the fibers compared to nuclear graphites.

*II.F.1.d. Breeder Materials.* Significant R&D efforts have been conducted in recent years with emphasis on the candidate ceramic breeder materials,  $\text{Li}_2$ ,  $\text{LiAlO}_2$ , and  $\text{Li}_4\text{SiO}_4$ . Mass transfer/weight loss of  $\text{Li}_2\text{O}$  in flowing helium at low moisture contents is a concern. Tritium release rates from ceramic breeders are sensitive to grain size and temperature. Small grain size in  $\text{LiAlO}_2$  is especially critical because of the low tritium diffusivity. At sufficiently high temperatures or

small grain size, most of the tritium should be released from all candidate ceramic breeder materials. There is a serious concern regarding stress corrosion cracking of austenitic steels by lithium salts and tritium recovery from the salt.

*II.F.1.e. Divertor Materials.* Primary candidate materials include tungsten plasma-facing materials bonded to copper heat sink. Liquid metals and helium burial concepts have been proposed as innovative divertor target materials. Vanadium, nickel, and iron are candidate materials for the helium burial concept. The minimum energy for effective helium trapping ( $\sim 30$  at. % trapping fraction) is estimated to be  $\sim 30$  to  $50$  eV. Analyses performed indicate that lithium and tin may be acceptable liquid-metal divertor targets.

*II.F.1.f. Magnet Materials.* The radiation limits for  $\text{Nb}_3\text{Sn}$  are estimated to be  $\sim 1 \times 10^{19}$  n/cm<sup>2</sup>. The dose limits for epoxy insulators and polyimide insulators are predicted to be in the range of  $\sim 1 \times 10^9$  and  $\sim 1 \times 10^{10}$  rad, respectively, depending on the shear stress requirements.

### II.F.2. Disruption Nuclear Analysis

Since disruptions have a major influence on the design and performance of the first wall and divertor, special emphasis was placed on analyses of these effects. A parametric erosion analysis was performed for the first-wall and divertor materials for a range of conditions. This analysis considered disruption times of 0.1 to 20 ms and deposited energy densities of  $\sim 100$  to  $1000$  J/cm<sup>2</sup> on stainless steel, graphite, and tungsten. The extent of vaporization, melt layer thickness for the metals, and effects of vapor shielding were determined. Based on a tentative disruption scenario in which thermal quench is assumed to occur in  $\sim 0.1$  ms with most of the energy going to the tungsten divertor plate, the predicted lifetime erosion of the tungsten is  $\sim 17$  mm and that of the steel wall is  $\sim 1.7$  mm. For this case, the melt layers are assumed not to erode in the short disruption times.

Analyses indicate that surface cracking of a steel wall will occur as a result of severe disruptions; however, propagation of the crack will not occur, and hence, the normal fatigue life will not be significantly degraded.

### II.F.3. First-Wall Designs

The first-wall design activity concentrated on evaluation of critical issues associated with a steel wall and a graphite-protected wall. The steel wall concept provides significant advantages with respect to design simplicity and lifetime under normal operating conditions. The primary concerns relate to vaporization and melting of the surfaces during a disruption. A graphite

liner will provide protection from severe disruptions; however, additional problems exacerbated during normal operation relate to more complex design, tritium retention in the graphite, and a limited radiation lifetime. A revised plasma disruption scenario developed during this phase has major implications regarding first-wall design.

Three first-wall design concepts were considered for in-depth analyses, using the modified INTOR design parameters to define performance characteristics and identify unresolved design issues. These analyses covered a wide range of reactor parameters including the reference operating conditions as given in Table II. The three designs have a water coolant with a Type 316 stainless steel structure. The first concept consists of a bare stainless steel water-cooled panel. The thickness of the plasma-facing panel is limited by thermal stress and/or fatigue criteria. The second concept uses a grooved structural wall to allow a higher erosion rate and surface heat flux relative to the first concept. The third concept has a radiatively cooled tile of graphite or carbon-carbon composite on the plasma side that will accommodate more severe disruption loads.

The bare stainless steel first wall is recommended as the reference for the INTOR design. The primary advantages of the bare steel wall include design simplicity and a well-established data base. Key issues identified for further study include (a) effectiveness of vapor shield during disruptions, (b) effects of disruptions on fatigue life, (c) melt layer stability during disruptions, and (d) advantages and disadvantages of cold-worked versus solution-annealed stainless steel, particularly as affected by welding/joining. For bare first-wall designs with a fatigue lifetime of  $2 \times 10^5$  cycles, the allowed peak nominal heat fluxes are  $\sim 0.4$

TABLE II  
INTOR Parameters for First-Wall/  
Blanket/Shield Analyses

Average neutron wall load (MW/m <sup>2</sup> )	1.3
Maximum surface heat flux to first wall (MW/m <sup>2</sup> )	0.2
Availability (%)	25
Number of cycles	$2 \times 10^5$
Cycle burn time (s)	$\geq 200$
Cycle time (s)	$\geq 270$
Number of major disruptions	200 to 1000
Peak disruption energy to inboard first wall (J/cm <sup>2</sup> )	175
Time for energy deposition per disruption (ms)	2
Sputtering erosion of stainless steel from first wall (mm/MW·yr/m <sup>2</sup> )	$\approx 0.2$
Tritium breeding blanket coverage	0.6 to 0.8



MW/m<sup>2</sup> for a thickness of ~6 mm. A thicker grooved wall will provide additional ruggedness.

*II.F.4. Tritium Breeding Blanket*

The primary objective of the blanket activity was to investigate the feasibility of providing tritium self-sufficiency without compromising the reactor design and reliability and with modest R&D requirements. Although several blanket concepts were examined, the analyses focused primarily on two concepts: (a) a water-cooled, ceramic breeder concept and (b) an aqueous/salt self-cooled concept. Both concepts utilize an austenitic steel structure, incorporate substantial amounts of beryllium to enhance the tritium breeding performance, and operate with low-temperature (~100°C) coolant.

The main function of the INTOR blanket is to produce the tritium required for operation with minimum first-wall coverage. The blanket extrapolation to commercial power reactor conditions and the proper temperature for power extraction have been sacrificed to achieve the highest possible local tritium breeding ratio (TBR) with minimum additional R&D and minimal impact on reactor operation. In addition, several other factors have been considered in the FWBS study including safety, reliability, lifetime, fluence, number of burn cycles, simplicity, cost, and development

issues. A set of blanket evaluation criteria has been compiled to compare possible INTOR blanket concepts.

The proposed INTOR blanket is a water-cooled, helium-purged system with layers of stainless steel structural material, beryllium multiplier, LiAlO<sub>2</sub> breeder, and carbon reflector (Fig. 3). The first-wall surface area for INTOR is 380 m<sup>2</sup> with 230 m<sup>2</sup> (~60%) coverage by the blanket. The total thickness of the breeder layers is ~60 mm, giving a breeder volume of 13.8 m<sup>3</sup>. The total thickness of the beryllium layers is ~240 mm, giving a multiplier volume of 55.2 m<sup>3</sup>. Assuming that the beryllium is at 70% of its theoretical density and the breeder is at 80% of its theoretical density gives masses of 71.4 Mg for beryllium and 28.9 Mg for LiAlO<sub>2</sub> (22.3 Mg for Li<sub>2</sub>O and 26.7 Mg for Li<sub>4</sub>SiO<sub>4</sub>).

Key design features for the water-cooled solid breeder blanket are the following:

1. high TBR
2. can utilize low-temperature (<100°C), low-pressure (<0.5 MPa) water coolant
3. provides safety and reliability advantages
4. utilizes ceramic breeder for which a data base is being developed

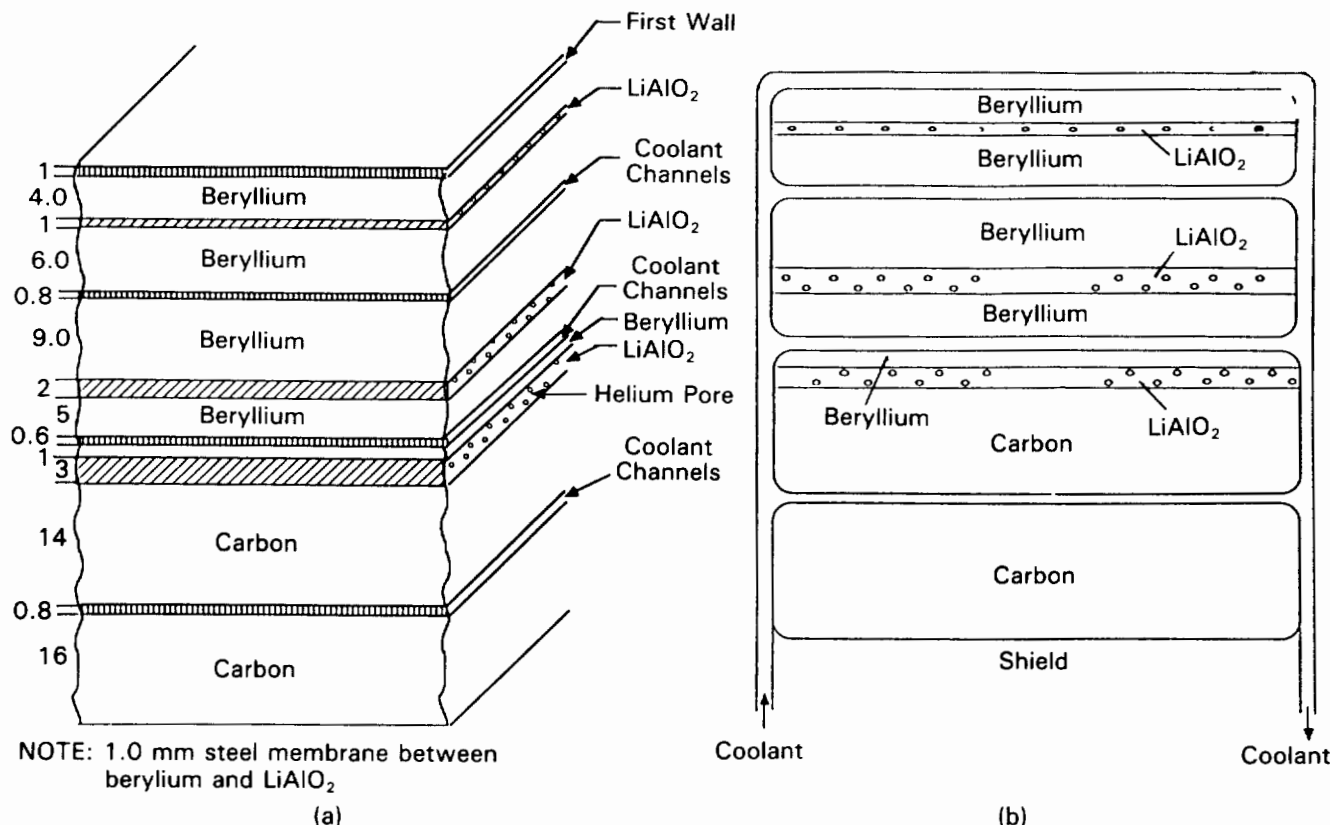


Fig. 3. Proposed INTOR blanket: (a) the blanket layers and (b) blanket coolant configuration.

5. low-temperature austenitic steel structure with low-pressure coolant provides low-technology system with minimum structure volume fraction
6. incorporates beryllium to provide high tritium breeding
7. low-temperature beryllium reduces swelling concerns.

It is concluded that tritium self-sufficiency is readily attainable if the key materials feasibility issues, i.e., aqueous stress corrosion and loss of fracture toughness of austenitic steel, can be favorably resolved.

#### *II.F.5. Nuclear R&D Needs*

Critical materials and technology R&D needs for the INTOR first wall, blanket, divertor, and shield were defined. The most important feasibility issues are aqueous stress corrosion of austenitic steel; effect of radiation on low-temperature fracture toughness of austenitic steel; and radiation effects on graphite and carbon-carbon composites (including helium).

#### **II.G. Engineering Issues**

Two topics are covered in the area of engineering issues: compact reactor concepts as tokamak concept innovations and engineering scoping studies performed in anticipation of a design upgrade of the INTOR concept.

##### *II.G.1. Compact Reactor Concepts*

A special area addressed in the INTOR Workshop was innovations that would significantly improve the prospects of tokamak development leading to an attractive, viable tokamak fusion reactor.

American scientists and engineers generated numerous ideas for consideration, including compact reactor concepts. Two ideas using copper coils were advanced. The first was the spherical torus, which is a very small aspect ratio confinement concept obtained by retaining only the indispensable components, such as the TF coils, inboard to the plasma torus. This concept is characterized by high toroidal beta ( $>0.2$ ), naturally large elongation ( $>2$ ), large plasma current ( $>7$  MA/tonne), strong paramagnetism, and strong magnetic helical pitch. This concept has features that combine to produce a spherical torus plasma in a unique physics regime that permits compact fusion at low field and modest cost. The second concept was the elongated tokamak concept, which calls for extreme shaping of the plasma by elongation ( $>4$ ). Benefits associated with this concept include good confinement, high beta, and high plasma current density at moderate magnetic fields and stresses. The high current density suggests the possibility of ohmic ignition. Maintenance and repair are facilitated using rapidly demountable TF coils.

Two ideas using superconducting magnet systems were also suggested. The first was an all-superconducting, steady-state tokamak based on a minimum major radius and strong plasma shaping. This concept relies on high magnet current densities, high-field plasma-shaping coils, minimum neutron shielding, and steady-state operations assuming current drive. The resulting design achieves high beta conditions in the first stability regime in a very compact device with associated modest cost. The concept is dependent on the development of efficient current drive methods. The second superconducting concept was the microwave tokamak. This idea seeks an attractive high- $Q$ , steady-state reactor in which the total plasma current is driven noninductively by a combination of electron cyclotron heating, wall reflection of synchrotron emission, and bootstrap current. The microwave sources need further development for this concept application.

Development of these concepts is not sufficiently advanced that they could be considered for a near-term device with INTOR-like objectives.

##### *II.G.2. Engineering Scoping Studies*

A series of scoping studies was performed for the eventual update of the INTOR design concept. They were initiated to learn which of many possible changes to the design would be feasible and practical and have a significant impact on the overall design and performance.

A set of recommended scoping studies was developed by all of the participants:

1. reduction in size and/or number of TF coils
2. single- versus double-null divertor
3. noninductive current drive
4. quasi-steady-state operation
5. pumped limiter with ergodic edge
6. combined use of NBI for heating, current drive, and impurity flow reversal
7. pusher coil for higher beta
8. higher plasma current
9. integration of the set individual elements.

In addition to these recommended elements, additional studies were performed in the United States to examine the impact of varying certain parameters and to develop a set of integrated point designs to illustrate possible upgrades to be considered for INTOR.

These scoping studies were performed using the Fusion Engineering Design Center tokamak systems code. This code has been used in numerous previous U.S. design studies and upgraded with time and application. The code has the ability to incorporate many physics and engineering variables and constraints. A

distinguishing feature of the present version is the ability to simultaneously iterate on many variables to achieve a converged solution for a selected FOM.

This study identified several high-sensitivity areas where significant impacts can be made on the design, and several representative integrated design concepts that indicate varying degrees of improvement that can be made to the INTOR design by making the indicated choices in configuration or engineering.

The following are ways to reduce the major radius:

1. increasing the elongation (to values in the 1.9 to 2.2 range)
2. using noninductive current drive (which permits reduction in the size of the solenoid)
3. reducing the inboard plasma scrape-off thickness
4. increasing the plasma operating temperature (to the 15- to 20-keV range)
5. reducing the inboard shield thickness
6. using higher overall TF coil current density at a given field level to reduce the TF coil thickness.

The results of these scoping studies provide a quantitative basis and insight for potential improvements in the INTOR design concept.

### III. ANALYSIS OF INTOR-LIKE DESIGNS

The IFRC recommended that the INTOR Workshop conduct critical analyses of existing INTOR-like designs during 1987, with the aim of preparing a useful information base for future design work for the Engineering Test Reactor (ETR). As a first step, members of the INTOR, Fusion Experimental Reactor (FER) (Japan), NET (European Communities), Test Fusion Reactor (OTR) (USSR) and Tokamak Ignition/Burn Experimental Reactor (TIBER) (United States) design teams met together in an IAEA specialists' meeting to document in a common format, discuss, and compare the program and technical objectives, the engineering and physics design constraints (i.e., physical limitations such as stress limits, beta limits), the main features that drive the design concept (i.e., choices made by the designers such as to incorporate noninductive current drive or a horizontal maintenance and assembly scheme), and the design specifications (e.g., major parameters, choice of materials, choice of heating method) for the five designs. These topics were further analyzed during the course of the INTOR Workshop.

There is much similarity in the objectives of the five designs. Achievement of reactor-relevant plasma operating conditions, incorporation of reactor-relevant technologies in the machine components, and provision for engineering testing are broad, common objec-

tives. All the designs are predicated on a start of construction of about 1993.

There are some differences in objectives, however. The fluence objective varies from  $0.3 \text{ MW} \cdot \text{yr}/\text{m}^2$  for FER to  $5.0 \text{ MW} \cdot \text{yr}/\text{m}^2$  for OTR, with associated variations in materials and component testing capabilities and availability requirements. Ignition is an objective for FER, INTOR, and NET, while steady-state operation at  $Q \geq 5$  is an objective for TIBER, and OTR has a high- $Q$  objective. Tritium self-sufficiency is an objective for OTR, while FER will not breed any tritium except in test modules. The OTR is the only design with a nuclear fuel production demonstration objective.

There is also a difference in the objective of the design studies, as distinct from the objectives of the devices, which has caused differences in the designs. The TIBER design activity had as an objective the study of the extent to which a compact design could be achieved by making aggressive assumptions about the development and incorporation of new technologies that are yet to be developed.

#### III.A. Physics Constraints

The physics assumptions and constraints for each of the four national ETR designs and INTOR are quite similar (Table III). The differences in the designs are mainly due to the choice and emphasis of different features (see Sec. III.C) and the use of different engineering constraints (see Sec. III.B). On the whole, the national designs tended to adopt more conservative physics assumptions than INTOR, especially with regard to beta and  $q_{edge}$ . All of the designs rely on H-mode confinement and have incorporated an open poloidal divertor for this reason. In addition, they rely on current scaling for confinement and beta, so that the specified currents are in the 10-MA range. The plasma is elongated to achieve this current. The elongations vary from 1.5 to 2.4. All of the designs have adequate margin for ignition with ASDEX-H scaling, but none of the designs can ignite with most L-mode scalings.

All of the designs rely on densities for ignited operation that are at the high end of the present tokamak data base. The designs utilizing current drive with subignited operation can afford more conservative assumptions with respect to the density limit. The Murakami parameters range from 15 to 25 for ignited operation and  $\sim 8$  for  $Q = 5$  operation.

All of the designs use a Troyon type of scaling for the beta limit, although the choice of the Troyon coefficient is somewhat different in each design. As stated before, this type of scaling leads each design to emphasize increased current as a way to maximize beta.

The edge safety factors vary among the designs, but the cylindrical safety factors are very similar for all of them.

TABLE III  
Physics Constraints

	INTOR	NET	FER	TIBER	OTR
$I$ (MA)	8	10.8	8.74	10	8
$I$	1.6	2.05	1.7	2.4	1.5
$\tau_E$ required (s)	1.4	1.9	1.7	0.44	1.7
$\tau_E$ (ASDEX-H) $\tau_E$ required	2.9	3.0	2.3	6.8	3
$n$ ( $10^{20}/\text{m}^3$ )	1.6	1.7	1.14	1.06	1.7
Murakami parameter <sup>a</sup> ( $10^{19}/\text{T}\cdot\text{m}^2$ )	19	23	15	8	25
Beta required (%)	4.9	5.6	5.3	6	3.2
Troyon coefficient (%)	4	3.5	3.5	2.8	3.5
Impurity control divertor	Single null	Double null	Single null	Double null	Single null
Pulse length (s)	150	350	800	55	600
Plasma heating method	ICRF	Tritium breeding	ICRF (LHCD rampup)	LHCD + NBI	ICRH

<sup>a</sup>Computed using line average density.

All of the designs rely on the operation of an open, high-recycling divertor to provide power and particle exhaust. Advanced fueling techniques, including high-velocity pellets and other schemes, have been incorporated in all.

A TF ripple in the range of 0.75 to 1.2% is anticipated to be adequate for fast alpha-particle confinement, although major uncertainties remain.

The physics assumptions for current drive and heating are quite similar among the designs. For those that do not rely on current drive, ICRF is generally the heating method adopted, insofar as a choice has been made. Where current rampup and transformer recharge is used, lower hybrid wave heating is the method of choice. Those designs incorporating steady-state current drive rely on 400- to 500-keV neutral beams for central current drive and lower hybrid waves for current drive at the edge. The penetration of lower hybrid waves is considered inadequate for high-density operation.

### III.B. Engineering Design Constraints

Engineering constraints are those parameters and limits used in a design that are derived primarily from physical laws of nature and over which the designer has limited control. These include such elements as the radiation damage limits and heat load limits. Choices made in one system or aspect of a design can then pose as a design limit to be satisfied by other systems or aspects of the design. For example, the decision to use a double-null, highly elongated plasma poses constraints on the mechanical configuration.

In the engineering category, the design constraints were arranged in three groupings: mechanical and configuration; electromagnetics, heating, and current drive technology; and nuclear.

#### III.B.1. Mechanical and Configuration Constraints

In the mechanical and configuration grouping, the major engineering design constraints and the range of choice used in the five designs are as follows:

1. magnet configuration: placement of all coils in a common cryostat or placement of magnets in a self-contained cryostat
2. method of reacting magnet loads: use of a bucking cylinder, wedging of the inner legs of the TF coils or reacting the TF coils directly from the central solenoid
3. vacuum boundary: use of a common boundary for the plasma and the magnets or the use of a separate vacuum containment for each system
4. number of replaceable modules: varies from 12 to 48, depending on the overall device configuration
5. component replaceability: Most of the designs assume that many of the components are designed to last the life of the device with no plan for replaceability; the other designs make no such assumption.
6. tritium breeding: varies from no tritium breeding (other than in test modules) to full tritium self-sufficiency
7. maintenance approach: horizontal or vertical removal of torus components
8. plasma configuration: varies from modestly elongated (1.5) single-null divertor plasmas to highly elongated (2.4) double-null divertor plasmas

9. radial dimensions: The five designs vary dramatically in the overall plasma major radius and in the thickness of the components and space allocations comprising the major radius. For example, the allowance for plasma scrape-off varies from 9 to 30 cm, the total inboard blanket/shield thickness varies from 48 to 105 cm, the accumulated allowance for assembly gaps and spaces varies from 2 to 20 cm, and the thickness of the TF coil inner leg varies from 49 to 110 cm.

### III.B.2. Electromagnetics, Heating, and Current Drive Technology

In the area of electromagnetics, heating, and current drive technology, the major differences are in the electromagnetics. All of the designs use similar heating and current drive technologies.

In the TF coil system, a number of different engineering design constraints are used. These are primarily related to the environment perceived to be necessary for the desired superconductor performance. These include the total and peak nuclear heating levels. The total nuclear heating level varies from  $\sim 8$  to 72 kW of nuclear heat deposition; the related peak nuclear heating levels vary from  $\sim 0.3$  to 5 kW/m<sup>3</sup>. Radiation protection requirements for the superconductor and the associated insulator also vary significantly; the radiation dose varies from  $\sim 2 \times 10^8$  to  $10^{10}$  rads. Other significant variables are the conductor current values (from 16 to 35 kA), the average winding pack current density (from  $\sim 10$  to 22 MA/m<sup>2</sup>), the magnetic energy (from 4 to 45 GJ), and the maximum quench voltage to ground (from  $\sim 7$  to 20 kV).

In the PF coil system, the dominant differences are related to the total volt-seconds the system must provide (from  $\sim 50$  to 210 V·s). In addition, there are differences in the allowable maximum field rate of change, varying from  $\sim 0.5$  to 3 T/s; differences in the OH current ramp time, from  $\sim 13$  to 30 s; differences in the breakdown voltage, from 10 to 35 s; and, finally, differences in the total magnetic stored energy, from  $\sim 4$  to 11 GJ.

### III.B.3. Nuclear Technology

In the nuclear systems area, there are significant differences in the engineering design constraints in the first wall and blanket, the divertor, and the shield area.

In the first-wall/blanket systems, these differences are related to the target lifetime fluence values (which range from 0.3 to 3 MW·yr/m<sup>2</sup>), the allowable stresses in the structural material (which are also tied to the number of lifetime cycles of operation), the tritium breeding requirement, the first-wall protection assumptions, and, finally, the assumptions related to the disruption scenario.

In the divertor area, the differences are related to the incorporation of different concepts for the physics and technology phases and to the differences in the disruption scenario.

In the shield area, the differences, therefore, are related largely to the need to protect the magnets and are tied to the allowable fluence to the superconductor, to the allowable dose to the insulators, and to the nuclear heating limits. A second constraint relates to the desire to minimize the overall thickness of the inboard shield region to minimize the size and cost of the design.

### III.C. Design-Driving Features

The five INTOR-like designs differ in a number of significant features, which tend to "drive" the characteristics of each design. Each of these design-driving features represents an aspect of the design where the designer has a choice among a number of options. These choices are compatible with the overall mission and supporting program and technical objectives established for each design.

The selection of each design-driving feature by each design team is also influenced by the judgment concerning important considerations related to each national program. These include the perceived timing for the necessary development and construction of each device, the perceived understanding of the present scientific and technological data base and the advances that can be made in the time period until the start of construction, and, finally, the maturity of the technology needed to support each design and its stated mission.

Table IV presents a comparison of the major design-driving features for the five INTOR-like designs. Many of these features are related to scientific desires and present understanding, which include the need to achieve ignition or not, the nature of the operating scenario (inductive or noninductive current drive, or some hybrid combination), the pulse length, the degree of plasma shaping (elongation), the type of impurity control (single- or double-null divertor), the nature of start-up, and the plasma heating method. The remaining major driving features result from operational and technological considerations, such as whether to breed tritium (and how much), the fluence target and the nature of the desired nuclear testing, and, finally, the approach to maintenance of the internal torus components (horizontal or vertical access).

### III.D. Systems Analysis

A systems analysis of the five INTOR-like designs (FER, NET, TIBER, OTR, and INTOR) was performed to evaluate and quantitatively determine the reasons for differences among the five designs and to determine the specific impact produced in a given design by a specific change. This quantitative analysis



TABLE IV  
Major Features of INTOR-Like Designs

Feature/Parameter	INTOR	NET	FER	TIBER	OTR
Major radius (m)	5.00	5.18	4.42	3.00	6.30
Minor radius (m)	1.20	1.35	1.25	0.83	1.50
Ignited or $Q$	Ignited	Ignited	$Q > 20$ to 30	$Q > 5$	$Q > 5$
Pulse length (s)	150.00	>200	800.00	Continuous wave	600.00
Impurity control	Single null	Double/single null	Single null	Double null	Single null
Operating scenario	Inductive	Inductive	Hybrid	Noninductive	Inductive
Elongation	1.60	2.20/1.60	1.70	2.40	1.50
Triangularity	0.25	0.70/0.30	0.20	0.40	0.30
Fluence objective ( $\text{MW} \cdot \text{yr}/\text{m}^2$ )	3.00	0.80	0.30	3.00	5.00
Tritium breeding	>0.60	>0.3	None	>1.0	>1.05
Plasma heating method	ICRH	(Tritium breeding)	(Tritium breeding)	NBI + LHCD	ICRH
Access for maintenance	Horizontal	Vertical	Horizontal	Horizontal	Horizontal

provides valuable insight into the way different choices affect a given design. The results should be valuable in the development of the next generation of tokamak designs.

### III.D.1. Systems Analysis Methodology

Systems analysis methodology has progressed significantly during the last several years. The capability has been developed to represent a tokamak point design and much of the complexity of the various systems comprising the design as well as their multiple interactions. Numerical optimization methods have been incorporated that enable simultaneous change of many variables subject to specified constraints. These features are incorporated into the Tokamak Engineering Test Reactor Analysis (TETRA) systems code.

### III.D.2. Replication of INTOR-Like Designs

A significant test of the systems analysis methodology is the ability to replicate various tokamak designs. A measure of the validity and usefulness of the methodology is the ability to reproduce the major features and performance of a variety of designs. One test is to use the systems analysis method to reproduce as accurately as possible (i.e., to replicate) the mechanical features, performance, physics parameters, and engineering parameters of an existing tokamak design. The systems analysis process requires input to be provided, which generates certain output. The TETRA code was used to replicate each of the five INTOR-like designs.

The results of these calculations demonstrate a good ability to accurately represent the general, as well as many specific, features and parameters of the designs. This demonstration provides confidence that parametric studies should provide meaningful indications of the impact of making a given change to a design.

### III.D.3. Sensitivity Analysis

Sensitivity calculations were performed relative to the TIBER design to determine the changes produced by deliberate changes in selected input. Calculations were performed in which one aspect of the design was changed (such as a mechanical feature or dimension, a physics assumption or parameter, or an engineering assumption or parameter). The impact on the design resulting from this single change was determined.

The results of this set of calculations allow an assessment of the items that have a high-leverage impact on the overall design and those that have considerably less impact. By performing a systematic assessment of the impact these items have on the design, the highest leverage items can be identified. Once identified, this information can be factored into the detailed design process and thereby provide guidance to the designers.

The results indicate that the parameters to which the design is most sensitive are energy multiplication factor  $Q$ , safety factor  $q$ , elongation,  $Z_{\text{eff}}$ , neutron wall load, and beta  $g$  coefficient (Troyon factor). The parameters to which the design is least sensitive are shield thickness, scrape-off layer (inboard) thickness, and plasma profiles.

There is an important distinction between parameter sensitivity and design impact. To draw practical conclusions from the sensitivity results, it is necessary to fold into the assessment the likely range of variation or uncertainty of a given parameter to determine the importance of a change in that parameter to the design. Parameters that have the greatest sensitivity will also have a large impact on the design even if the range of variation of that parameter is not large. However, parameters that have the least sensitivity could still have a large impact on the design if the range of variation or uncertainty in that parameter is large. This practical consideration should be recognized in the design process.

Calculations were also performed in which a collection of items was changed. For example, it was of interest to determine the effect of substituting, at one time, all physics-related assumptions made in one design into a second design. It was also of interest to examine the effect of making similar collective changes of the engineering assumptions or specifications of the general features of the design (design-driving features).

Differences in the individual assumptions of the INTOR-like designs can be grouped together into categories such as physics, engineering, or features. The physics category includes beta and beta coefficient, safety factor, ignition margin, plasma temperature and density, edge ripple, and plasma profile factors. The engineering category includes dimensions of components (OH and TF coils, bucking cylinder, shield, etc.), stress levels, radiation dose levels, and gaps. The features category includes plasma configuration (elongation and triangularity), maintenance approach, fluence level, tritium breeding, single- or double-null divertor, and operating scenario.

These studies were performed in a manner similar to the individual sensitivity studies. For example, studies were performed in which a calculational transition was made from the INTOR design to the TIBER design and from the NET design to the TIBER design.

The results indicate that the transition from one design to another can be made. This successfully demonstrates the ability to substitute global groupings of changes (all physics, engineering, or features) and make the transition from one design to another.

No single FOM seems to exist that should be used to best measure the impact of sensitivity calculations. Valuable measures include major radius and cost. However, for a given design, the impact of changes must still be interpreted with caution because the changes may also imply impacts on less measurable design aspects such as the risk associated with the design, new technology developments or new physics, maturity or technology changes, or different timing relative to construction.

#### *III.D.4. Relative Cost Estimates*

There is an ongoing and important interest in the way the estimated capital cost is affected by various aspects of tokamak design. In any international comparison study, the various national designs are costed by each country using the national procedure to account for engineering fabrication, transportation, installation, and project management costs. These national approaches are all different, not only in the units of currency used, but in the ways the various cost elements are treated in the costing process. Recognizing these differences, a cost comparison was performed by the United States for each of the five INTOR-like designs to determine the relative ranking of capital cost and to later compare with similar information generated by the other INTOR participants.

The relative capital costs were normalized to the INTOR cost estimate. The results indicate the following:

1. The costs for INTOR and NET are approximately the same.
2. The costs for FER are ~10% less than the cost of INTOR.
3. The costs for TIBER are ~35% less than the cost of INTOR.
4. The costs for OTR are ~40% greater than the cost of INTOR.

These relative cost comparisons must be interpreted with care because the various designs make different assumptions about the timing of construction, the amount of supporting R&D required, and the aggressive or conservative posture regarding the maturity of the technology in the design. Factoring these considerations into the design can alter these cost comparisons, perhaps dramatically.

#### *III.D.5. Conclusions of Systems Analysis*

Overall, this comparative systems analysis has demonstrated that valuable insights can be derived from such analyses, which can be performed rapidly at little cost. The results can provide valuable guidance to the evolution of any given design. In this sense, such analyses are of high interest and value in the early stages of the design to provide rapid evaluation of many options. Generation of such a design data base of information at the early stages of the design establishes a strong quantitative support base for initial choices among options. Such choices permit the design team to focus quickly and engage in more detailed design efforts based on a reasonably established initial baseline design.

### **IV. IMPLICATIONS FOR THE INTOR DESIGN CONCEPT**

The principal conclusions from the work of Phase 2A, Part 3, and their implications for the INTOR design are summarized.

#### **IV.A. Impurity Control**

Modeling studies and experimental data still support the choice of a poloidal divertor for impurity control and a high- $z$  (tungsten) divertor collector plate surface. Thus, the major aspects of the recommended impurity control system are the same as in the reference INTOR design concept. A number of modifications to the INTOR design concept may be necessary, however. A low- $z$  limiter for start-up may be required. If the present uncertainty regarding the severity of disruptions remains, it may be prudent to install protective armor on the first wall, at least during the initial phase. The value of  $Z_{eff}$  may have to be increased

from 1.5 to 2.0, in which case allowance would have to be made for a corresponding increase in the power radiated to the first wall.

#### IV.B. Operational Limits and Confinement

A variety of H-mode energy confinement scaling laws have been proposed over the last years. On the basis of these laws, the INTOR design concept is considered to have adequate confinement capability to achieve ignition, if there is no substantial degradation with heating power.

The INTOR design concept somewhat exceeds both the Murakami-Hugill limit and the Greenwald density limit, but it should be noted that these limits are exceeded by as much as a factor of 2 in experiments with intense auxiliary heating. Thus, the density in INTOR is very probably below the actual density limit.

Analytical and experimental results indicate that the Troyon beta limit  $g$  factor must be reduced from the value of 4 used in the INTOR design concept to 3.0 to 3.5 and that the safety factor  $q_I$  must be increased from 1.8 to at least 2. Because

$$\beta (\%) = \frac{g I_p (\text{MA})}{a (\text{m}) B (\text{T})}$$

and

$$q_I = \frac{5 \left\{ \frac{1}{2} \left[ 1 + \left( \frac{b}{a} \right)^2 \right] \right\}^{1/2} B (\text{T}) a^2 (\text{m})}{R (\text{m}) I_p (\text{MA})},$$

a combination of increasing the plasma current, the magnetic field, and the plasma elongation ( $b/a$ ) and/or reducing the major radius in the INTOR design concept is probably necessary to achieve the performance objective (e.g., neutron wall load).

#### IV.C. Current Drive and Heating

There is now a substantial experimental and theoretical data base on noninductive current drive (by lower hybrid waves or neutral beams, or a combination of both) so that it can be considered as an option to achieve the performance objectives of INTOR. However, the predicted efficiency is low and the required power may be of the order of 100 MW even if the plasma parameters are optimized for current drive. Thus, while inductive current drive is retained as the reference option in the present INTOR design concept, noninductive current drive is suggested for use in a new INTOR-like design concept, provided that such a design could be shown to be feasible and to have substantial advantage over an inductively driven design.

New experimental data support the previous choice of ICRH as the reference heating scheme in INTOR. However, if neutral beams and lower hybrid waves were chosen for current drive in a new INTOR-like design concept, it would be appropriate to use them

also for heating (and in the case of neutral beams, for added impurity control by flow reversal).

#### IV.D. Electromagnetic

It was established that the active control coils should be located inside the TF coils and outside the shield. Also, it was confirmed that the first-wall/blanket structure is adequate for passive stabilization.

Modeling studies indicate that the INTOR PF coil system could be designed more optimally. In particular, the coils should be placed closer to the midplane. Leaving a large midplane window for horizontal access imposes a moderate penalty in terms of stored energy for small to moderate plasma elongation, but a large penalty for highly elongated plasmas.

#### IV.E. Configuration and Maintenance

The reference INTOR maintenance concept is horizontal removal of large torus segments, which requires that a rather large window for access be left at the midplane, with the consequence that no PF coils can be located near the midplane. Analysis of this maintenance scheme and comparison with a vertical or oblique removal concept led to the conclusion that the simpler maintenance procedures associated with horizontal maintenance outweigh the penalty in PF coil optimization for small to moderate plasma elongation, but that the vertical or oblique maintenance scheme is preferable for moderate to large plasma elongation, for which the penalty in PF coil optimization becomes too large. Thus, if the plasma elongation must be increased to  $>2$ , as may be necessary to satisfy the plasma operating limits (see Sec. IV.B), then a change from the horizontal maintenance concept to the vertical or oblique concept may be required. A combination of the two concepts might also have its merits.

For the reference INTOR maintenance concept, a transfer cask for containing tritium and dust is recommended for personnel access to the reactor hall. Because of recent developments, an *in situ* maintenance scheme is recommended for plasma-facing components (e.g., protective tiles on the first wall).

The use of iron inserts to reduce the field ripple would enable a reduction of  $\sim 50$  cm in the TF coil bore or a reduction in the number of coils from 12 to 10, without significantly complicating the configuration. Thus, the use of iron inserts is recommended.

#### IV.F. First Wall and Blanket

Analyses of the divertor collector plate, the first wall, and the breeding blanket confirm the choices that were made in the INTOR design concept. The reference divertor plate concept of tungsten tiles bonded to a water-cooled copper heat sink is predicted to have a lifetime of  $2 \times 10^4$  cycles, limited during normal burn by fatigue and erosion. This implies that the divertor plate must be replaced ten times during the lifetime of INTOR. A bare, water-cooled austenitic stainless steel

first wall is still recommended, unless new information indicates that the frequency of disruptions would be much greater than is assumed in the present disruption scenario.

The reference breeding blanket concept, with ceramic breeding material, an austenitic stainless steel structure, and water cooling, is still recommended. It is possible to use water at relatively low pressure, which is recommended for better reliability.

It was found that a beryllium multiplier together with certain design stratagems can be used to achieve a TBR greater than unity and hence to make INTOR self-sufficient in tritium production without increasing the inboard dimension or the level of risk. Accordingly, it is recommended that INTOR be equipped with a nonreactor-relevant tritium-producing blanket adequate to provide tritium self-sufficiency.

#### IV.G. Design Sensitivity

Systems analyses indicate that the size and cost of an INTOR-like design is very sensitive to the ignition margin  $Z_{eff}$ , the plasma elongation, the safety factor, the value of the  $g$  factor in the Troyon beta limit, the neutron wall load, the shield attenuation, and the allowable stress in the TF coils. Thus, the size and cost of INTOR could be reduced by future developments that would lead to improved energy confinement, improved impurity control, stability at larger plasma elongation, lower safety factor, larger values of the Troyon  $g$  factor, a higher limit of radiation damage on the magnet insulators, and magnet structural materials operating at higher stress levels.

#### ACKNOWLEDGMENTS

The work summarized in this paper was performed by many scientists and engineers working in U.S. laboratories, universities, and industry under the guidance of the authors. These contributors are listed in Ref. 5, where the detailed report of the work is presented. Their contributions are gratefully acknowledged.

#### REFERENCES

1. INTOR Group, "International Tokamak Reactor: Zero Phase," STI/PUB/556, International Atomic Energy Agency (1980); see also *Nucl. Fusion*, **20**, 349 (1980).
2. INTOR Group, "International Tokamak Reactor: Phase One," STI/PUB/619, International Atomic Energy Agency (1982); see also *Nucl. Fusion*, **22**, 135 (1982).
3. INTOR Group, "International Tokamak Reactor: Phase Two A Part I," STI/PUB/638, International Atomic Energy Agency (1983); see also *Nucl. Fusion*, **23**, 1513 (1983).
4. INTOR Group, "International Tokamak Reactor: Phase Two A Part II," STI/PUB/714, International Atomic Energy Agency (1986); see also *Nucl. Fusion*, **25**, 1791 (1985).
5. W. M. STACEY et al., "U.S. Contribution to the Phase 2A, Part 3 INTOR Workshop, 1985-88," Georgia Institute of Technology (1988).
6. W. M. STACEY et al., "The U.S. Contribution to the International Tokamak Reactor Workshop," Georgia Institute of Technology (1979); see also W. M. STACEY et al., "INTOR—A First Generation Tokamak Experimental Reactor," *Nucl. Eng. Design*, **63**, 171 (1981).
7. W. M. STACEY et al., "The U.S. Contribution to the International Tokamak Reactor Phase-1 Workshop," Georgia Institute of Technology (1980).
8. W. M. STACEY et al., "The U.S. Contribution to the International Tokamak Reactor Phase-1 Workshop," Georgia Institute of Technology (1981); see also W. M. STACEY et al., "U.S. Conceptual Design Contribution to the INTOR Phase 1 Workshop," *Nucl. Technol./Fusion*, **1**, 486 (1981).
9. W. M. STACEY et al., "U.S. FED-INTOR Activity and U.S. Contribution to the International Tokamak Reactor Phase 2A Workshop," Georgia Institute of Technology (1982); see also W. M. STACEY et al., "The FED-INTOR Activity," *Fusion Technol.*, **4**, 202 (1983).
10. W. M. STACEY et al., "U.S. Contribution to the Phase 2A, Part 2 INTOR Workshop, 1983-1985," Georgia Institute of Technology (1985); see also W. M. STACEY et al., "U.S. Contribution to the Phase 2A, Part 2 International Tokamak Reactor Workshop, 1983-1985, June 1985," *Fusion Technol.*, **11**, 316 (1987).
11. M. ONO et al., *Applications of Radio-Frequency Power to Plasma*, pp. 155, 230, 270, 274, S. BERNBEI and R. W. MOTLEY, Eds., American Institute of Physics, New York (1987); see also M. ONO et al., *Phys. Rev. Lett.*, **60**, 294 (1988).
12. R. J. HAWRYLUK et al., "TFTR Plasma Regimes," *Proc. 11th Int. Conf. Plasma Physics and Controlled Nuclear Fusion Research*, Kyoto, Japan, November 13-20, 1986, p. 51, International Atomic Energy Agency (1987).
13. T. NAGASHIMA et al., *Applications of Radio-Frequency Power to Plasma*, pp. 94, 115, 282, S. BERNBEI and R. W. MOTLEY, Eds., American Institute of Physics, New York (1987).
14. D. A. EHST et al., *Nucl. Eng. Design/Fusion*, **2**, 305 (1985); D. A. EHST et al., *Nucl. Eng. Design/Fusion*, **2**, 319 (1985); and D. A. EHST et al., *Nucl. Eng. Design/Fusion*, **3**, 113 (1985).
15. C. F. F. KARNEY and N. J. FISCH, "Current in Wave-Driven Plasmas," *Phys. Fluids*, **29**, 180 (1986).
16. *Proc. Specialists' Mtg. Noninductive Current Drive*, NET-PM-86-003, Max-Planck-Institut für Plasmaphysik (1987) and IAEA-TECDOC-441, International Atomic Energy Agency (1987).
17. D. A. EHST and K. EVANS, Jr., *Nucl. Fusion*, **27**, 1267 (1987).
18. F. X. SÖLDNER, in *Applications of Radio-Frequency Power to Plasmas*, S. BERNBEI and R. W. MOTLEY, Eds., American Institute of Physics, New York (1987).